Genome-wide analysis of gene expression in neuroblastomas detected by mass screening.

Alexander Krause, Valérie Combaret, Isabelle Iacono, Bruno Lacroix, Christelle Compagnon, Christophe Bergeron, Sandrine Valsesia-Wittmann, Philippe Leissner, Bruno Mougin, Alain Puisieux

Genome-wide analysis of gene expression in neuroblastomas detected by mass screening

Alexander Krause[a1], Valérie Combaret[b], Isabelle Iacono[b], Bruno Lacroix[a], Christelle Compagnon[a], Christophe Bergeron[b], Sandrine Valsesia-Wittmann[b], Philippe Leissner[a], Bruno Mougin[a], Alain Puisieux[b2]

[a] *Human Genetics Department, bioMérieux SA, 69280 Marcy l'Etoile, France,*

[b] *Centre Léon Bérard, 69008 Lyon, France and Université Lyon I, Faculté de Pharmacie, 8 avenue Rockefeller, 69008 Lyon [A.P].*

A.K. and V. C. equally contributed to this work

[1] This work was supported, in part, by a Marie Curie research fellowship (to A.K., QLK2-1999-50537) from the European Commission.

[2] Corresponding author:

Alain Puisieux
Centre Léon Bérard
Unité d'Oncologie Moléculaire
28 rue Laënnec, 69008 Lyon, France
Phone: + 33 (0)4 78 78 26 67
FAX: + 33 (0)4 78 78 28 21
e-mail: puisieux@lyon.fnclcc.fr

Abstract

Neuroblastoma (NB) is the most common extracranial solid tumor of childhood and the third most common pediatric cancer. Although numerous factors including patient age, disease stage and genetic abnormalities have been shown to be predictive of outcome, the mechanisms responsible for the highly variable clinical behavior of this tumor remain largely unknown. In order to gain new insights into the biology of this tumor, we performed microarray analysis and compared the gene expression patterns of NB detected by mass screening, characterized by highly probable spontaneous regression, versus stage 4 NB with poor prognosis. The bioinformatics analysis revealed a set of 19 discriminatory genes that may play a significant role in the natural progression of the disease. Validation of these results and further mechanistic studies would shed new light on the biology of tumor progression, and provide new tools to predict clinical outcome in children with NB.

Key words: Neuroblastoma; Mass screening; Expression profiling; Outcome prediction.

1. Introduction

Neuroblastoma is the most common extracranial solid neoplasm in children. The clinical hallmark of NB is heterogeneity, with a clinical behavior ranging from spontaneous regression to tumor progression and metastasis (1). The prognosis of NB depends on patient age and disease stage at diagnosis. In general, children diagnosed before 1 year of age and/or with localized disease are curable with surgery and little or no chemotherapy. It is known that some of these tumors may undergo spontaneous regression or differentiate into ganglioneuromas (2). In contrast, the majority of patients over 1 year of age develop locally aggressive and/or metastatic disease that is ultimately fatal. Early detection has thus been considered a promising approach to improve NB outcome. Consequently, several countries such as Japan, Canada and European countries (3) have implemented mass screening programs measuring urinary catecholamine metabolites among infants under 12 months of age, with the aim of detecting unfavorable NB at an early stage. Although focal genetic alterations were observed in a fraction of tumors from mass-screened patients (4), all programs led to substantial over-diagnosis among screened participants, with no decrease in overall mortality from the disease. This led to the suggestion that the majority of cases diagnosed by screening would have experienced spontaneous regression, without ever developing the disease (5). This was confirmed by further clinical studies, particularly a pilot study consisting of a "wait and see" observation of infants with NB detected by mass screening before any surgery or chemotherapy (6). Strikingly, more than 60% of stage 1 or 2 NB detected by mass screening regressed spontaneously. In order to better characterize the different subtypes of neuroblastomas, we analyzed the transcriptional pattern of approximately 10,000 genes in both NB detected by mass screening and metastatic NB clinically diagnosed in older children. This analysis was performed using Affymetrix chips.

2. Materials and methods

2.1. Tumor samples

Twenty-three human NB samples were collected according to the institutional review board guidelines of the Centre Léon Bérard (CLB, Lyon, France). All tumor samples were obtained at the time of diagnosis, prior to any treatment. Tumors were classified according to the International NB Staging System (INSS). We first performed a genome-wide gene expression analysis of 17 well-characterized tumors, 10 NB obtained by mass screening and 7 stage 4 NB detected in older children, to define genes differentially expressed in each group. Histologically, all tumors were described as undifferentiated NB. Subsequently, another six tumors were analyzed to test the predictive power of each classifier identified. Table 1 summarizes clinicopathological parameters of the patients included in the study.

2.2. Detection of the percentage of malignant cells by immunostaining

Immunochemical staining was performed using an indirect three-stage immunoenzymatic procedure with alkaline phosphatase, as previously described (7). Briefly, air-dried slides (cryostat sections or cytocentrifuged smears) were fixed for 5 minutes with acetone at 4°C and incubated for 60 minutes with monoclonal antibodies (MoAbs) at appropriate dilution, then for 30 minutes with enzyme-conjugated rabbit anti-mouse immunoglobulins and for 30 minutes with enzyme-conjugated swine anti-rabbit immunoglobulins. Washes were performed with Tris buffer. The final step consisted of a 15-minute incubation with Naphtol-As-Mx phosphate, dimethylformamide, levamisole, and Fast Red (Sigma, St Louis, MO). Slides were counterstained with hematoxylin, mounted permanently with glycerin, and evaluated under an optical microscope. Neuroblastoma cells were quantified by immunostaining with anti-CD56 or NB84. All enzyme-conjugated

immunoglobulins anti-CD56 and anti–human neuroblastoma NB84 were purchased from Dakopatts (Copenhagen, Denmark). Cytologic or histologic analyses were performed in parallel on each specimen using standard techniques.

2.3. Microarray hybridization

Trizol reagent was used to extract total RNA from surgical specimens or bone marrow punctures (Table 1). Following purification on Qiagen RNeasy columns (Qiagen, Hilden, Germany), the integrity and quality of the total RNA was assessed on an Agilent 2100 Bioanalyzer (Agilent Technologies, Waldbronn, Germany) by means of the RNA 6000 Nano Assay (Agilent). cDNA synthesis, cRNA *in vitro* transcription, labeling and fragmentation, as well as the hybridization of target cRNAs to U95Av2 microarrays were performed according to the manufacturer's instructions (Affymetrix, Santa Clara, CA). A transcriptional pattern of approximately 10,000 genes was studied. The Microarray Suite 5.0 software (MAS5.0, Affymetrix) was used to process and normalize scanned raw data.

2.4. Data analysis

In an initial step, the microarray raw data analyzed in this study were normalized using the Microarray Suite 5.0-software (Affymetrix). Normalized array data from 10 NB obtained by mass screening and 7 stage 4 NB with poor prognosis (“training set”) then served to define a set of discriminatory genes (Table 1). The identified gene classifier was subsequently used to analyze six additional tumor samples (“test set”). Gene selection and class prediction were performed by means of the PAM algorithm (prediction analysis for microarrays algorithm), which is an enhanced variant of the nearest-centroid classifier (8). This method identifies genes differentially expressed in two or more tumor types, and simultaneously ranks the determined genes according to their importance to the classifier.

Moreover, the PAM algorithm also estimates the prediction error in the classification by 10-fold cross-validation. Prior to the PAM analysis, we performed three filtering steps on the abundant microarray raw data in order to eliminate uninformative genes whose expression does not vary significantly between the two tumor groups. Firstly, we removed all probe sets that the Affymetrix Microarray Suite 5.0 software consistently considered "absent" in all 17 training samples, implying that the genes associated with these probe sets were not transcribed in the examined NB. Secondly, we filtered out all genes with average expression levels below a minimal threshold of 500 fluorescence units. The final preselection step excluded all genes whose average expression levels varied by less than 30% between the two groups. The 1,488 probe sets retained were subjected to PAM analysis. The algorithm identified a combination of 27 probe sets allowing accurate classification of the 17 tumors of the training set. In order to further reduce the number of genes necessary to classify NB, we only retained genes with a low family-wise error rate as calculated by the Bonferroni method ($p>0.05$) (9). This very conservative correction for multiple testing stringently decreases the number of false positive genes in array analyses. Tumor classification probabilities for the training and test sets were calculated by a leave-one-out cross-validation method independent from the PAM algorithm (Fig. 1). The R Statistical Software package and PAM implementation used in this study were downloaded from *www.r-project.org*.

2.5. Primer design, cDNA synthesis, and real-time quantitativeRT- PCR

To confirm the results of microarray experiments, the mRNA expression levels of genes were analyzed by quantitative RT-PCR based on SYBR green fluorescence. Gene-specific PCR primer sequences were determined by means of the Primer3 or Primer Express softwares (Table2). For cDNA templates, 1 µg of total RNA was converted into cDNA using a first-strand DNA synthesis kit (Amersham France). After 6-fold dilution, 2.5 µl of cDNA

were used for real-time PCR and mixed with the forward and reverse primers (300 nM) and SYBR Green Master Mix buffer. The volume of the reaction mixture was 15 µl. PCR amplification was carried out in 96-well microtiter optical plates using ABI Prism 7000 Sequence Detection System (Applied BioSystem USA). The reference gene (HPRT1) was analyzed in the same experiment as the target gene. Following a 10-min denaturation at 95°C, gene amplification was performed as follows: 40 cycles at 95°C for 15 s and at 60°C for 1 min. The experiments were performed in duplicate to ensure reproducibility of the technique. Quantification was performed using both the standard curve method and the comparative C_T method as recommended by the manufacturer. Standard curves were constructed in each PCR run and gene expression was determined using these standard curves. Serial log dilutions of cDNA obtained from neuroblastoma cell lines were used as template for the standard curves. The relative expression of the target gene was defined by comparison with the expression of the reference gene. Pearson's and Spearman's rank tests were used to calculate the correlation between microarray and quantitative RT-PCR expression signals (Table 3).

3. Results and discussion

Mass screening for NB at 6-12 months of age has led to a striking increase in the prevalence of tumors in the screened populations. However, this did not seem to correlate with a decreased prevalence of NB in patients older than 1 year of age or those with stage 4 disease and, consequently, with a decrease of mortality from the disease. These disappointing findings ultimately led to reconsider the policy of mass screening for NB. Many children diagnosed with NB by screening underwent unnecessary treatments for tumors that would regress spontaneously. However, screening programs also allowed to collect specific subsets of cancer samples. In order to gain insight into the molecular pathways underlying the different subtypes of the disease, we performed microarray analysis by means of U95Av2 GeneChips (Affymetrix) on 10 NB detected by mass screening and 7 stage 4 NB, all collected in France, and compared the gene expression patterns of the two sets. From a total of over 10,000 genes tested, the bioinformatics analysis of array raw data discriminated 200 genes with a differential expression between the 2 groups analyzed (data not shown). The advanced selection study performed as described in the "material and methods" section further identified a discriminatory set of 19 genes (Table 3). The Bonferroni adjustment used to pinpoint the most significant differences between the two data sets efficiently decreased the rate of false positive genes in the gene list, while being more permissive for false negative genes. This shortcoming of the Bonferroni correction, however, was acceptable in view of the concise and non-exhaustive character of the proposed gene signature.

Real-time RT-PCR confirmed the relevance of microarray data. By studying tumors of the training set, we demonstrated that 12 of the 19 genes analyzed showed a significant correlation using both Pearson's and Spearman's correlation tests, while three additional genes

proved to be correlated using Spearman's rank test (Table 3). Pearson's and Spearman's tests also evidenced a correlation of the latter 3 genes when tumors of the test set were included.

Identified genes have been related to various biochemical and biological processes, including pre-mRNA splicing (*RNPS1*, *SNRPB*, *PTBP1*), transcriptional regulation (*RUVBL2*, *TIF1β*, *SSRP1*), control of cell proliferation and differentiation (*IGFBP7*, *UBE2C*, *PMP22*), cell adhesion (*EPB41L3*, *COL6A3*), angiogenesis (*SPARC*), DNA-repair (*FEN1*) or carbohydrate metabolism (*FUCA1*). The classifier contains several genes previously shown to be deregulated in human cancers. Among those, some genes that are under-expressed in tumors detected by screening are known to display oncogenic activities. For example, UBE2C/UbcH10 belongs to the family of ubiquitin-conjugating enzymes (E2). It has been shown to promote cell growth by mediating the proteolytic destruction of mitotic cyclins A and B, thereby allowing the onset of anaphase in mammalian cells (10). Interestingly, *UBE2C/UbcH10* is highly expressed in various primary tumors such as uterine, stomach, bladder and lung tumors, as compared with matched normal tissues (10). *In vitro*, *UBE2C/UbcH10* overexpression causes accelerated growth, increased saturation density and the promotion of anchorage-independent growth, which supports its oncogenic role in a wide variety of human tumors. Our observation suggests that UBE2C/UbcH10 may play a similar role in aggressive NB. Notably, *RUVBL2* and *TIF1β*, two of the genes identified in the present study, are known to act as transcriptional cofactors of c-myc, a factor involved in transcription regulation, responsible for both activation and repression. In association with other proteins such as TRRAP, hGCN5, BAF53, and TIP49, RUVBL2 (TIP48/TIP49b), which possesses ATPase/helicase activity, binds to the transactivation domain of c-myc. These proteins are thought to remodel the chromatin to activate or repress the gene expression linked to c-myc (11). TIF1β protein (TRIM28, KAP-1), like *TRIM2*, is a member of the

tripartite motif family. Members of this family display a specific motif including three zinc-binding domains, a RING, a B-box type 1 and a B-box type 2, and a coiled-coil region. *TIF1β* mediates transcriptional control by interacting with the Kruppel-associated box repression domain found in many transcription factors. It was recently shown that *TIF1β* can recruit an HDAC (histone deacetylase) complex to c-myc (12). Based on the present observation of *RUVBL2* and *TIF1β* overexpression in aggressive NB, it would be worthy to analyze the relationship of the two gene products with the MYCN oncoprotein.

Several genes with lower expression in aggressive NB than in tumors detected by mass screening were previously identified as potential tumor suppressor genes. Among those, the *FUCA1* (alpha-L-fucosidase) gene was recently shown to be down-regulated in NB with unfavorable characteristics (13). The role of *FUCA1* in tumor progression remains unclear, but we may speculate that its inactivation perturbs the glycosylation of proteins involved in cell adhesion and promotes cancer cell invasion and metastasis. *FUCA1* is located in 1p34, a region frequently deleted in various human cancers, including NB (14). *EPB41L3* (*DAL-1*) shares significant homology with members of the 4.1/ezrin/radixin/moesin/neurofibromatosis (4.1 ERM/NF2) protein family. Like other members of this family, EPB41L3 is localized to the plasma membrane near points of cell-cell contact, and is involved in the control of cell adhesion, cellular growth and differentiation. The EPB41L3 gene has been shown to be down-regulated in considerable portions of lung carcinomas, and the restoration of its expression significantly suppresses cell growth *in vitro* (15). Furthermore, the EPB41L3 gene is localized to chromosome band 18p11.3, which undergoes frequent loss of heterozygosity in breast or astrocytic tumors and meningiomas, indicating that EPB41L3 inactivation may have broad implications in tumor development (16). COL6A3, a component of type VI collagen, is also involved in cell adhesion. A significant down-regulation of the 3 polypeptides required

for the assembly of type VI collagen was previously reported in most of the cell lines derived from mesenchymal tumors, including fibrosarcomas, rhabdomyosarcomas, leiomyosarcomas, chondrosarcomas and liposarcomas (17). It has been suggested that the absence of this important adhesion protein may contribute to tumorigenicity, invasiveness and/or metastasis. PMP22 (GAS-3) gene product is a dual function protein involved in both peripheral nerve myelination and cell proliferation. In fibroblasts, its expression is regulated through the cell cycle, being at its highest during growth arrest (18). Initially defined as a marker of Schwann cells, this gene was recently shown to be down-regulated in *MYCN*-expressing NB (19). IGFBP-7 (IGFBP-rP1/mac25/angiomodulin) is a member of the low-affinity IGFBP family (insulin-like growth factor binding proteins). The role of IGFBP-7 in carcinogenesis is probably complex and remains under investigation. Several reports indicate that it acts as a negative regulator of cell proliferation; its expression has been observed to be down-regulated in breast cancers through different mechanisms including gene mutation and deletion, hypermethylation of CpG islands in the promoter region or increased protein degradation (20). However, *IGFBP-7* expression is up-regulated in uterine leiomyomas and colorectal cancers, where it is a powerful predictor of cancer aggressiveness and poor outcome (21). IGFBP-7 might exert an oncogenic activity through its potential role in tumor angiogenesis and in the modulation of vascular functions. Similarly, the precise biological functions of the SPARC protein remain unclear. SPARC plays a modulatory role in cell-matrix interactions and contributes to vascular morphogenesis and cellular differentiation. However, contradictory reports regarding the role of SPARC in cell growth and tumor formation suggest that its effects are cell type-specific. Indeed, in ovarian cancer, SPARC decreases cell growth rate, induces apoptosis and reduces tumorigenicity, whereas the experimental inactivation of SPARC abrogates the tumorigenicity of melanoma cells. More recently, Chlenski and colleagues have demonstrated that SPARC potently inhibits angiogenesis and

impairs NB growth *in vitro* (22). The high expression of SPARC observed in NB detected by mass screening may thus be an important element of the favorable evolution of these tumors.

The observation of the relatively low expression of potential oncogenes and high expression of potent tumor suppressor genes in NB detected by mass screening as compared to clinically diagnosed tumors is concordant with previous studies reporting that tumors detected by mass screening displayed favorable biological features (1). In this context, the pattern of *FEN1* expression was unexpected. FEN1 (flap endonuclease) is a DNA repair and replication endonuclease and exonuclease that has been shown to play a critical role for maintaining genomic integrity. Mutations of *FEN1* may give rise to a number of genetic diseases, such as myotonic dystrophy, Huntington's disease, ataxias, fragile X syndrome, whereas *FEN1* haploinsuffiency leads to cancer progression (23). Although *FEN1* was recently identified as a potent *MYCN* target gene (24), the cause and biological consequences of its apparent overexpression in clinically diagnosed NB remain to be elucidated.

Clinical as well as biological observations have clearly demonstrated that NB encompasses several different diseases. Genetic features such as ploidy, *MYCN* copy number and deletion of 1p can help discriminate between aggressive tumors and those that are likely to regress or differentiate. It remains unclear whether these NB subsets originate from different cells or represent different genetic evolutionary pathways, but current evidence supports that they are genetically distinct and that most biologically favorable tumors do not evolve into aggressive ones. By comparing the gene expression profiles of NB detected by mass screening and of clinically diagnosed tumors, we have identified genes whose expression may play a significant role in the natural progression of the disease. This approach has also allowed to define a limited list of genes differentially expressed in favorable (NB detected by mass

screening) as compared to unfavorable (stage 4 NB) cases. In order to test the potential prognostic impact of the 19-gene classifier we analyzed, in a preliminary approach, six independent localized NB. Five patients were still alive and in complete remission (median follow-up 10 years), whereas one relapsed and died 10 months after diagnosis (Table 1). While tumors from patients in complete remission showed a gene expression pattern similar to that of tumors obtained by mass screening, the expression profile of the unfavorable NB sample was comparable to that of metastatic tumors (Figure 1). This preliminary observation suggests that the identified classifier may predict tumor aggressiveness in NB. The validation of these results, as well as further mechanistic studies, would shed new light on the biology of tumor progression, and provide new tools for predicting outcome in children with NB.

Acknowledgements

This work was supported by grants from the Comité de l'Ain de la Ligue contre le Cancer.

References

[1] G.M. Brodeur, Neuroblastoma: Biological insights into a clinical enigma, Nat. Rev. Cancer 3 (2003) 203-216.

[2] T. Iwanaka, K. Yamamoto, Y. Ogawa, M. Arai, M. Ito, H. Kishimoto, R. Hanada,S. Imaizumi, Maturation of mass-screened localized adrenal neuroblastoma, J. Pediatr. Surg. 36 (2001) 1633-1636.

[3] R. Erttmann, T. Tafese, F. Berthold, R. Kerbl, J. Mann, L. Parker, F. Schilling, P. Ambros, H. Christiansen, M. Favrot, H. Kabisch, B. Hero, T. Philip, 10 years' neuroblastoma screening in Europe: preliminary results of a clinical and biological review from the Study Group for Evaluation of Neuroblastoma Screening in Europe (SENSE), Eur. J. Cancer 34 (1998) 1391-1397.

[4] R. Kerbl, C.E. Urban, I.M. Ambros, H.J. Dornbusch, W. Schwinger, H. Lackner, R. Ladenstein, V. Strenger, H. Gadner, P.F. Ambros, Neuroblastoma mass screening in late infancy: insights into the biology of neuroblastic tumors, J. Clin. Oncol. 21 (2003) 4228-4234.

[5] F.H. Schilling, C. Spix, F. Berthold, R. Erttmann, J. Sander, J. Treuner, J. Michaelis, Children may not benefit from neuroblastoma screening at 1 year of age. Updated results of the population based controlled trial in Germany, Cancer Lett. 197 (2003) 19-28.

[6] A. Yoneda, T. Oue, K. Imura, M. Inoue, K. Yagi, K. Kawa, M. Nishikawa, S. Morimoto, M. Nakayama, Observation of untreated patients with neuroblastoma detected by mass screening: a “wait and see” pilot study, Med. Pediat. Oncol. 36 (2001) 160-162.

[7] M.C. Favrot, V. Combaret, E. Goillot, E. Tabone, E. Bouffet, D. Dolbeau, R. Bouvier, C. Coze, J. Michon, T. Philip, Expression of leucocyte adhesion molecules on 66 clinical neuroblastoma specimens, Int. J. Cancer 48 (1991) 502-510.

[8] R. Tibshirani, T. Hastie, B. Narasimhan, G. Chu, Diagnosis of multiple cancer types by shrunken centroids of gene expression, Proc. Natl. Acad. Sci. USA 99 (2002) 6567-6572.

[9] M.L. Wayne, L.M. McIntyre, Combining mapping and arraying: An approach to candidate gene identification, Proc. Natl. Acad. Sci. USA 99 (2002) 14903-14906.

[10] Y. Okamoto, T. Ozaki, K. Miyazaki, M. Aoyama, M. Miyazaki, A. Nakagawara, UbcH10 is the cancer-related E2 ubiquitin-conjugating enzyme, Cancer Res. 63 (2003) 4167-4173.

[11] M.A. Wood, S.B. McMahon, M.D. Cole, An ATPase/helicase complex is an essential cofactor for oncogenic transformation by c-Myc, Mol. Cell 5 (2000) 321-330.

[12] A. Satou, T. Taira, S.M. Iguchi-Ariga, H. Ariga, A novel transrepression pathway of c-Myc. Recruitment of a transcriptional corepressor complex to c-Myc by MM-1, a c-Myc-binding protein, J. Biol. Chem. 276 (2001) 46562-46567.

[13] M. Ohira, A. Morohashi, H. Inuzuka, T. Shishikura, T. Kawamoto, H. Kageyama, Y. Nakamura, E. Isogai, H. Takayasu, S. Sakiyama, Y. Suzuki, S. Sugano, T. Goto, S. Sato, A. Nakagawara, Expression profiling and characterization of 4200 genes cloned from primary neuroblastomas: identification of 305 genes differentially expressed between favourable and unfavourable subsets, Oncogene 22 (2003) 5525-5536.

[14] G. Schleiermacher, M. Peter, J. Michon, J.P. Hugot, P. Vielh, J.M. Zucker, H. Magdelenat, G. Thomas, O. Delattre, Two distinct deleted regions on the short arm of chromosome 1 in neuroblastoma, Genes Chromosomes Cancer 10 (1994) 275-281.

[15] Y.K. Tran, O. Bogler, K.M. Gorse, I. Wieland, M.R. Green, I.F. Newsham, A novel member of the NF2/ERM/4.1 superfamily with growth suppressing properties in lung cancer, Cancer Res. 59 (1999) 35-43.

[16] A.L. Charboneau, V. Singh, T. Yu, I.F. Newsham, Suppression of growth and increased cellular attachment after expression of DAL-1 in MCF-7 breast cancer cells, Int. J. Cancer 100 (2002) 181-188.

[17] B. Trueb, B.F. Odermatt, Loss of type VI collagen in experimental and most spontaneous human fibrosarcomas, Int. J. Cancer 86 (2000) 331-336.

[18] C. Karlsson, M. Afrakhte, B. Westermark, Y. Paulsson, Elevated level of gas3 gene expression is correlated with G0 growth arrest in human fibroblasts, Cell Biol. Int. 23 (1999) 351-358.

[19] M. Alaminos, J. Mora, N.K. Cheung, A. Smith, J. Qin, L. Chen, W.L. Gerald, Genome-wide analysis of gene expression associated with MYCN in human neuroblastoma, Cancer Res. 63 (2003) 4538-4546.

[20] G. Landberg, H. Ostlund, N.H. Nielsen, G. Roos, S. Emdin, A.M. Burger A. Seth, Downregulation of the potential suppressor gene IGFBP-rP1 in human breast cancer is associated with inactivation of the retinoblastoma protein, cyclin E overexpression and increased proliferation in estrogen receptor negative tumors, Oncogene 20 (2001) 3497-3505.

[21] Y. Adachi, F. Itoh, H. Yamamoto, Y. Arimura, Y. Kikkawa-Okabe, K. Miyazaki, D.P. Carbone, K. Imai, Expression of angiomodulin (tumor-derived adhesion factor/mac25) in invading tumor cells correlates with poor prognosis in human colorectal cancer, Int. J. Cancer 95 (2001) 216-222.

[22] A. Chlenski, S. Liu, S.E. Crawford, O.V. Volpert, G.H. DeVries, A. Evangelista, Q. Yang, H.R. Salwen, R. Farrer, J. Bray, S.L. Cohn, SPARC is a key Schwannian-derived inhibitor controlling neuroblastoma tumor angiogenesis, Cancer Res. 62 (2002) 7357-7363.

[23] M. Kucherlapati, K. Yang, M. Kuraguchi, J. Zhao, M. Lia, J. Heyer, M.F. Kane, K. Fan, R. Russell, A.M. Brown, B. Kneitz, W. Edelmann, R.D. Kolodner, M. Lipkin, R. Kucherlapati, Haploinsufficiency of Flap endonuclease (Fen1) leads to rapid tumor progression, Proc. Natl. Acad. Sci. USA 99 (2002) 9924-9929.

[24] E.A. Raetz, M.K. Kim, P. Moos, M. Carlson, C. Bruggers, D.K. Hooper, L. Foot, T. Liu, R. Seeger, W.L. Carroll, Identification of genes that are regulated transcriptionally by Myc in childhood tumors, Cancer 98 (2003) 841-853.

Table 1: *Clinical characteristics of the twenty-three neuroblastoma tumors analyzed*

Patient	Age at Diagnosis [months]	Stage	Sample origin	Histology[a]	Percentage of malignant cells	MYCN amplification[b]	1p status[b]	Index ploidy	Clinical feature[c]	Status[d]	
Training set											
1	6.5	4s	Adrenal gland	NB	90	NA	D	2.3	MS	Alive	(10)
3	7	4s	Adrenal gland	NB	70	NA	ND	1	MS	Alive	(10)
4	7	2	Adrenal gland	NB	85	NA	ND	1.4	MS	Alive	(10)
5	6	2	Sympathetic ganglion	NB	90	NA	ND	1.9	MS	Alive	(10)
10	15	1	Adrenal gland	NB	90	NA	D	1.4	MS	Alive	(5)
11	5.5	2	Thorax	NB	80	NA	ND	1.5	MS	Alive	(8)
12	6	1	Adrenal gland	NB	85	NA	ND	1.8	MS	Alive	(8)
13	1.5	1	Adrenal gland	NB	95	NA	ND	1.4	MS	Alive	(7)
14	4	2b	Cervico-thorax	NB	95	NA	ND	1.8	MS	Alive	(7)
15	0.5	4s	Adrenal gland	NB	90	NA	ND	1.7	MS	Alive	(2.2)
2	28	4	Bone marrow	NB	80	A	D	NT	UF	Alive	(13)
6	80	4	Bone marrow	NB	95	A	D	NT	UF	Dead	(3.5)
7	10.5	4	Adrenal gland	NB	90	A	D	1	UF	Dead	(1.1)
9	54	4	Bone marrow	NB	80	NA	ND	NT	UF	Dead	(2)
17	106	4	Bone marrow	NB	50	NA	ND	NT	UF	Alive	(1.5)
18	43	4	Adrenal gland	NB	80	NA	D	NT	UF	Dead	(0.9)
19	18	4	Adrenal gland	NB	80	A	D	0.9	UF	Alive	(1.2)
Test set											
Test-1	21	1	Adrenal gland	GGNB	60	NA	D	1.4	F	Alive	(10)
Test-2	16	1	Adrenal gland	NB	80	NA	ND	1.5	F,MS	Alive	(6)
Test-3	14	2	Cervical	NB	80	NA	ND	1.8	F	Alive	(12)
Test-4	18	2a	Thorax	GGNB	85	NA	NT	NT	F	Alive	(5)
Test-5	21	2b	Adrenal gland	NB	90	A	D	NT	UF	Dead	(0.8)
Test-6	7	4s	Thorax	NB	80	NA	ND	NT	F	Alive	(13)

[a] NB designates neuroblastoma and GGNB stands for ganglioneuroblastoma
[b] MYCN-amplification was detected by Southern blotting and FISH-analysis. The 1p status was detected by RFLP and/or FISH analysis. (+) corresponds to "expressed" and (-) to "not expressed".
[c] "MS" designates patients detected by mass screening, while "F" stands for a favorable and "UF" for an unfavorable clinical prognosis
[d] Patient follow-up (in years) is given between parentheses.
Abbreviations: A= amplified, NA= not amplified, D = deleted, ND = not deleted, NT = not tested

Table 2 : *Primers used for real-time RT-PCR analysis of the 19 genes differentially expressed in neuroblastomas detected by mass screening vs. neuroblastomas of unfavorable clinical outcome*

		Forward (sense primer)	Reverse (antisense primer)
2062_at	IGFBP7	5'-TGTCCTCATCTGGAACAAGG-3'	5'-GGCAGGAGTTCTGTCCTTTG-3’
38077_at	COL6A3	5'-TGTAGAAGCTCCGGGTGTAGATTC-3'	5'-ACACATTAGCACCATACTGATAGGTCAT-3'
41385_at	EPB41L3	5'-GTTGGACCCTGCTAAGGAAA-3'	5'-CAGATAGTTGGGCAGGGTCT-3'
41814_at	FUCA1	5'-AAAGAGGCGCTGCTCACTGT-3'	5'-AGAGAAGTTCGTTGATTATAGTGATGGTA-3'
671_at	SPARC	5'-CACATTAGGCTGTTGGTTCAAACT-3'	5'-CAGGATGCGCTGACCACTT-3'
33353_at	FLJ30781	5'-TTTACATCCAGAGGCACGAC-3'	5'-CACGATGTCAGCAAACAGG-3'
38653_at	PMP22	5'-GACCCAGTGCATCCAACAGA-3'	5'-GTGTGCGCGTAAAGCTTCAC-3'
34877_at	JAK1	5’-TGCCCAGAAGCAGTTCAAGA-3’	5’-TCCGAACCGTGCAGACTGTA-3’
39382_at	TRIM2	5'-CAGTAACAACCAATGTGTGCAG-3'	5'-TGCCAAAACGACTTTTGAAC-3'
33443_at	TDE2	5'-GGCGAGCTGGATACCATGTT-3'	5'-CACTAGGACAGCATCGGCATAG-3'
38984_at	KIAA0436	5’-ACAGCACCAGTGTTTTCGAG-3’	5’-TGTTTCCAATTCCCAGTTGA-3’
36186_at	RNPS1	5'-GCCCCGGCTGCAGAA-3'	5'-CCAGAAAACCGGAGGGAATC-3'
38455_at	SNRPB	5'-GCTGGACCGGAAGTAGGTTTCT-3'	5'-GCCGCTACCGGAAATGC-3'
33425_at	TIF1β	5'-CAGGAAGGCTATGGCTTTGG-3'	5'-CCGTTTCACACCTGACACATG-3'
37739_at	SSRP1	5'-CGCCAGATGTTCTTTGTGATCA-3’	5'-CAGGAAGTGGTAGCGAGTTTGG-3'
35758_at	RUVBL2	5'-CATGCTGGACATCGAGAGCTT-3'	5'-GGACAGGCGCCATGTCA-3'
40593_at	PTBP1	5'-CGCTGCGCATCGACTTT-3'	5'-GTAGTCACGGCTCTTGTCATTGTT-3'
1516_g_at	FEN1	5’-ACCCCGAACCAAGCTTTAG-3’	5’-CAACACAGAGGAGGGATGAC-3’
1651_at	UBE2C	5'-TCCTCACGCCCTGCTATCA-3'	5'-TTCAGGATGTCCAGGCATATGT-3'
reference gene	HPRT1	5'-CACTGGCAAAACAATGCAGACT-3'	5'-CGACCTTGACCATCTTTGGATT-3'

Table 3: *Set of 19 genes differentially expressed between neuroblastomas detected by mass screening and. neuroblastomas of unfavorable clinical outcome*

Probe set[a]	Gene symbol	Fold change[b]	p-value[c]	Pearson's test[d] (p value)	Spearman's test[d] (p value)	Chromosomal location	Description
2062_at	IGFBP7	-5	0.0000003	0.0977	0.004	4q12	IGF-binding protein 7
38077_at	COL6A3	-5	0.0021	0.0011	<0.0001	2q37	Collagen type VI, alpha 3 chain
41385_at	EPB41L3	-5	0.00003	0.0606	0.0123	18p11.32	Erythrocyte membrane band 4,1-like 3
41814_at	FUCA1	-5	0.000049	0.0531	0.0246	1p34	Tissue alpha-L-fucosidase 1
671_at	SPARC	-5	0.014	0.0163	0.0008	5q31.3-q32	SPARC / Osteonectin
33353_at	FLJ30781	-3.3	0.0000008	0.001	<0.0001	7p13-p12	cDNA clone FLJ30781 fis
38653_at	PMP22	-3.3	0.0017	0.0079	0.0021	17p12-p11.2	Peripheral myelin protein 22
34877_at	JAK1	-2.5	0.00000002	0.0436	0.0078	1p31.3	Janus Kinase 1
39382_at	TRIM2	-2.5	0.00000004	0.232	0.2983	4q31.3	Tripartite motif-containing 2
33443_at	TDE2	-2	0.0003	0.019	0.0006	6q22.33	Tumor differentially expressed 2
38984_at	KIAA0436	-2	0.00022	0.4373	0.2657	2p22.1	Putative neutral amino acid transporter
36186_at	RNPS1	1.6	0.0036	0.1157	0.088	16p13.3	RNA binding protein S1
38455_at	SNRPB	1.7	0.04	0.503	0.0664	20p13	Small nuclear ribonucleoprotein B/B1
33425_at	TIF1β	1.8	0.00001	0.0058	0.0428	19q13.4	Transcription intermediary factor 1β
37739_at	SSRP1	2	0.00009	0.0042	<0.0001	11q12	Structure specific recognition protein 1
35758_at	RUVBL2	2.1	0.00006	0.0002	0.0027	19q13.3	RuvB-like DNA helicase TIP49b
40593_at	PTBP1	2.1	0.0004	0.0004	<0.0001	19p13.3	Polypyrimidine tract binding protein 1
1516_g_at	FEN1	2.7	0.022	<0.0001	<0.0001	11q12	Endonuclease for 5' FLAP-structures
1651_at	UBE2C	2.9	0.015	<0.0001	<0.0001	20q13.11	Ubiquitin-conjugating enzyme E2 C

[a] Affymetrix probe sets as used by the GeneChip U95Av2-microarray.

[b] Fold changes obtained from microarray analysis between unfavorable and mass-screening neuroblastomas. A negative value indicates a down-expression in unfavorable neuroblastomas whereas a positive value indicates an overexpression in unfavorable neuroblastomas.

[c] p-value calculated on the basis of 12,625 probe sets represented on the U95Av2 microarray, using the Bonferroni correction for multiple testing.

[d] Pearson's and Spearman's rank tests were used to calculate the coefficient of correlation between microarray and quantitative RT-PCR expression signals. $P<0.05$: significant correlation.

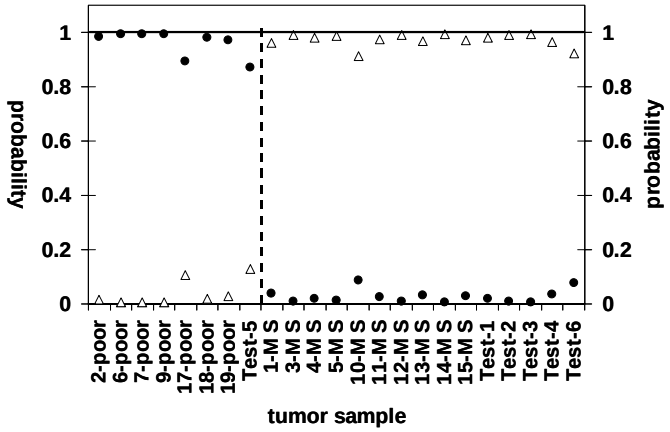

Figure 1. *Cross-validated classification of the 23 neuroblastomas using the identified set of 19 genes.*

The identified 19-gene classifier allows accurate segregation between NB detected by mass screening (MS) and NB of unfavorable clinical outcome. The vertical axis indicates the probability of tumor classification as calculated in a leave-one-out cross-validation approach, with triangles (Δ) representing the probability for tumors of being of favorable and circles (●) of unfavorable clinical outcome according to the expression of the 19 genes. For example, poor prognosis was assigned to tumor #17 with a probability of around 90%. The "Test"-tumors depicted are specimens of blinded outcome whose clinical prognosis could be correctly predicted using the classifier (cf. Table 1). The dashed vertical line separates NB of unfavorable outcome from NB detected by mass screening.